ISSN: 1813-4890

Analysis of Spatiotemporal Variation of Vegetation Net Primary Productivity in the Northeast Forest-Grassland Ecotone of China

Dongchang Liu, Aruhan*

College of Desert Control Science and Engineering, Inner Mongolia Agricultural University, Hohhot, 010018, China.

*Corresponding author: Aruhan

Abstract

This study examines the Northeast China forest-grassland ecotone using the Carnegie-Ames-Stanford Approach (CASA) model to calculate vegetation Net Primary Productivity (NPP) from 2000-2023. We integrated meteorological data, vegetation parameters, and remote sensing imagery to analyze spatiotemporal patterns of NPP dynamics throughout this critical transition zone. The research provides scientific evidence for regional carbon sink management strategies and contributes to a deeper understanding of carbon sequestration mechanisms in these ecologically sensitive areas. Our findings offer theoretical foundations and technical support for climate change mitigation and ecosystem management optimization, demonstrating both academic significance and practical value for environmental policy development and implementation.

Keywords

Forest grass ecotone, Net primary productivity, Temporal and spatial characteristics, Drivers.

1. Introduction

Since the Industrial Revolution, human activities have dramatically increased greenhouse gas emissions such as CO_2 and CH_4 from terrestrial ecosystems, rapidly elevating atmospheric greenhouse gas concentrations and intensifying the Earth's surface greenhouse effect. This enhancement of downward radiation has triggered significant imbalances in the global climate system [1]. The resulting frequent extreme climate events—including glacier melting, sea level rise, land desertification, and food crises—pose serious threats to human survival and ecological security [2]. These changes represent substantial dangers to global ecosystems and human society. As a core component of the carbon cycle, terrestrial ecosystems play a crucial role in regulating atmospheric CO_2 concentrations and mitigating climate change [3]. Therefore, systematic research on terrestrial ecosystem carbon cycling processes and their spatial distribution characteristics not only helps accurately assess global carbon budgets but also provides scientific basis for formulating climate policies and improving ecological compensation mechanisms.

Carbon, as an essential constituent element of terrestrial ecosystems, is widely distributed in nature in various forms, with its cycling processes closely related to human survival and development [4]. Terrestrial ecosystems, serving as significant carbon reservoirs, store carbon in soil organic carbon, inorganic carbon, vegetation biomass, litter, and dead plants [5]. Vegetation constitutes the core of terrestrial ecosystems, playing a vital role in global carbon cycling and energy flow while serving as a sensitive indicator for monitoring environmental changes across multiple scales [6]. In the context of global warming, plant photosynthesis is significantly affected by rising temperatures and extreme climate events such as droughts and floods, leading to dynamic changes in land-atmosphere carbon fluxes and CO_2 concentrations.

Soil, as the world's largest organic carbon reservoir, accounts for 67%-75% of global carbon stocks, substantially exceeding the combined total of vegetation and atmospheric carbon pools [7]. However, due to complex underlying surface structures and the synergistic effects of multiple natural and anthropogenic factors, terrestrial ecosystems exhibit significant spatiotemporal heterogeneity and uncertainty in carbon cycling processes [8]. Simultaneously, human disturbances to carbon pools have exacerbated ecosystem vulnerability, producing important feedback effects on global climate change [9].

Net Primary Productivity (NPP) is defined as the net accumulation of organic carbon fixed by green plants through photosynthesis within specific spatiotemporal scales after deducting autotrophic respiration consumption. It serves as a core indicator for measuring ecosystem carbon assimilation capacity [10]. Current NPP estimation methods primarily include statistical models, process models, and parameter models, with their methodological evolution and regional applicability becoming international research hotspots. Therefore, accurately assessing NPP—the dynamic balance between carbon sinks and sources [11]—and systematically analyzing its spatiotemporal differentiation patterns and evolutionary trends provides not only important basis for scientifically formulating carbon sink management policies but also establishes theoretical foundations and practical guidance for addressing climate change challenges and promoting green, low-carbon transformation and sustainable development.

The Northeast China forest-grassland ecotone, as a typical region for global change research, demonstrates high sensitivity to climate change in its ecosystems. This region features diverse vegetation types, including forests, grasslands, and farmlands, with ecosystem carbon sink functions jointly influenced by climate, topography, and human activities [12]. Research indicates that this ecotone has recently exhibited strong carbon sink potential. However, its carbon balance state shows significant response characteristics to seasonal climate changes, manifested as dynamic regulatory imbalances between respiration and photosynthesis [13]. Observational data show that over the past 20 years, the average spring and autumn temperatures in the Northern Hemisphere have risen by 1.1°C and 0.8°C, respectively. Autumn warming has induced a 28.6% increase in vegetation respiration rates, significantly shortening the carbon sink action period, while enhanced spring photosynthesis has extended the carbon sink effect [14]. Additionally, this region frequently experiences extreme weather events, such as summer droughts and winter cold spells, further exacerbating inter-annual NPP fluctuations [15].

Therefore, this study focuses on the Northeast China forest-grassland ecotone, using annual NPP data along with topographic, meteorological factors, and human activity data. Employing trend analysis methods, we examine the spatiotemporal variation patterns of vegetation NPP across different study areas to provide scientific basis for regional carbon sink management. This research not only helps deepen understanding of carbon sink mechanisms in the Northeast forest-grassland ecotone but also offers theoretical support and technical underpinning for addressing climate change and optimizing ecosystem management, demonstrating significant academic value and practical implications.

2. Material and methods

2.1. Study area

The The Northeast Forest-Grassland Ecotone (NFGE) is situated at the transitional interface between the forest boundaries of the Yanshan and Greater Khingan Mountains and adjacent grasslands, encompassing approximately 520,000 km². This region is positioned between 39°30′-53°20′N and 113°50′-126°04′E, spanning parts of Zhangjiakou and Chengde cities in Hebei Province, and portions of Tongliao, Hulunbuir, Chifeng, and Xing'an League in Inner

Mongolia Autonomous Region.Climatologically, the NFGE represents a transition zone between temperate semi-humid monsoon and temperate semi-arid continental climate systems, with an east-to-west precipitation gradient (500-600 mm to 300-400 mm), significant temperature variations, and well-defined seasonality.Geomorphologically, the northern section is dominated by the Greater Khingan Mountains (500-1,500 m elevation), while the southern portion features the Yanshan Mountain range. The central area consists of hills and plateaus, transitioning to grassland plains westward. Major river systems include the Nenjiang and West Liaohe, with microtopographical features such as sand dunes, lakes, and wetlands distributed throughout.Soil types transition from east to west, progressing from brown soils to black soils and chestnut soils, with sandy soils in areas like the Horqin sandy land. Vegetation patterns include coniferous-broadleaved mixed forests in the east, coniferous forests in the northern Greater Khingan region, and steppe formations in western sections. The forest-grassland interface features distinctive shrub communities dominated by Corylus heterophylla and Lespedeza bicolor.The NFGE exhibits ecological vulnerability characterized by environmental sensitivity, complex community structures, and elevated land degradation risk. The region is sparsely populated, with an economy based primarily on animal husbandry and forestry. As a critical ecological barrier and biodiversity hotspot in China, effective management must consider its ecotonal characteristics and implement site-specific conservation approaches.

2.2. Data Sources

2.2.1. NDVI Data

This study utilizes the MOD13A1 product to obtain Normalized Difference Vegetation Index (NDVI) data. This product provides vegetation index values at 500-meter spatial resolution, comprising two primary vegetation layers: the Normalized Difference Vegetation Index (NDVI) and Enhanced Vegetation Index (EVI). NDVI serves as a continuity index of the National Oceanic and Atmospheric Administration's Advanced Very High Resolution Radiometer (NOAA-AVHRR) data, while EVI is specifically designed to enhance sensitivity in high biomass regions. The MOD13A1 product employs an optimization algorithm that selects pixels with minimal cloud cover, optimal viewing angles, and maximum NDVI/EVI values from a 16-day observation period.

The data processing workflow included: (1) converting HDF format data acquired from the NASA EARTHDATA official website to GeoTIFF format; (2) conducting spatial mosaicking of tiled data; (3) applying the Maximum Value Composite (MVC) method to synthesize 16-day data into monthly maximum values; (4) performing regional clipping based on the Northeast forest-grassland region vector boundary; and (5) standardizing data projection to the WGS1984 coordinate system

2.2.2. NPP Validation Data

To validate the accuracy of the model estimation results, this research employed the MODIS/Terra Net Primary Productivity (NPP) product (MOD17A3) from 2000 to 2023, provided by the National Aeronautics and Space Administration (NASA). This dataset features a spatial resolution of 500 meters and a temporal resolution of 8 days. The data acquisition and processing workflow remained consistent with that of the NDVI data, ensuring uniformity of validation data with model input data in terms of spatial resolution and processing methodology, effectively reducing validation bias caused by data processing disparities.

2.2.3. Vegetation Type Data

Vegetation type information was derived from the MODIS land cover product MOD12Q1. This product integrates multispectral reflectance data from both Terra and Aqua satellites, employing supervised classification methods complemented by post-processing techniques and auxiliary information to optimize classification results, providing annual global land cover

ISSN: 1813-4890

type distribution at 500-meter resolution. The MOD12Q1 product encompasses multiple classification systems, with this study adopting the International Geosphere-Biosphere Programme (IGBP) classification scheme to categorize regional vegetation into forests, shrublands, grasslands, and other types.

Data processing included: (1) converting HDF format data to GeoTIFF format; (2) performing spatial mosaicking; (3) maintaining 500-meter spatial resolution during resampling; (4) clipping based on the study area vector boundary; and (5) standardizing projection to the WGS1984 coordinate system.

2.2.4. Solar Radiation Data

Solar radiation data were sourced from the TerraClimate global high-resolution climate dataset. TerraClimate provides monthly climate and water balance data for global land surfaces from 1958 to 2023, with a spatial resolution of 4 kilometers (approximately 1/24 degree), offering crucial high spatiotemporal resolution inputs for ecological and hydrological studies at global scales.

This study utilized the solar radiation data subset, with the processing workflow as follows: (1) converting NetCDF (NC) format data to GeoTIFF format; (2) performing spatial mosaicking; (3) applying bilinear interpolation to resample 4-kilometer data to 500 meters, maintaining consistent spatial resolution with other input data; (4) conducting regional clipping based on the Northeast forest-grassland region vector; and (5) standardizing projection to the WGS1984 coordinate system. During the resampling process, particular attention was paid to preserving the physical significance of radiation values and avoiding anomalous values introduced by interpolation.

2.2.5. Temperature and Precipitation Data

Temperature Data:This study employed the "Monthly Mean Temperature Dataset for China at 1km Resolution (1901-2023)," featuring a spatial resolution of 0.0083333 degrees (approximately 1 kilometer) and a temporal span from January 1901 to December 2023, with data units in 0.1°C. This dataset was generated for the Chinese region through the Delta spatial downscaling approach, based on the global 0.5-degree climate dataset released by the Climate Research Unit (CRU) and the global high-resolution climate dataset released by WorldClim. Data quality has been validated using 496 independent meteorological observation stations, confirming high reliability and accuracy of the dataset.

Precipitation Data:Precipitation data were derived from the "Monthly Precipitation Dataset for China at 1km Resolution (1901-2023)," featuring spatial resolution consistent with the temperature data at 0.0083333 degrees (approximately 1 kilometer). This dataset was similarly generated using the Delta spatial downscaling method based on CRU and WorldClim datasets and validated using 496 independent meteorological observation stations. The original data, stored in NetCDF format, underwent processing procedures consistent with other data to convert to the same spatial reference system as other input data.

Both meteorological datasets underwent the following processing workflow: (1) converting NetCDF format data to GeoTIFF format; (2) clipping based on the study area; (3) applying bilinear interpolation for resampling to 500-meter resolution, maintaining consistency with other data; and (4) standardizing projection to the WGS1984 coordinate system. The high-resolution characteristics of these meteorological data provided essential support for accurate modeling of regional vegetation productivity.

Through the integration and synchronized processing of these datasets, this research established a spatiotemporally consistent, uniformly resolved multi-source remote sensing data input system, laying a solid data foundation for accurate estimation of vegetation primary productivity.

2.3. .NPP estimation model method

This study employed the Carnegie-Ames-Stanford Approach (CASA) model[16], which utilizes remote sensing satellite imagery as its foundational data source. The model critically integrates two key parameters in the photosynthetic process: Absorbed Photosynthetically Active Radiation (APAR) and light use efficiency (ε). By transforming the calculation of APAR and light use efficiency into a quantitative analysis of environmental factors—including normalized difference vegetation index (NDVI), precipitation, temperature, and solar radiation—the CASA model has emerged as a sophisticated and widely adopted methodology for estimating Net Primary Productivity (NPP) within light use efficiency models.

This approach not only demonstrates the theoretical advantages of parameterized models in remote sensing ecology but also provides a precise and operationally robust technical pathway for assessing productivity in complex ecological systems.The calculation formula is as follows:

$$\mathrm{NPP}(x,t) = \mathrm{APAR}(x,t) \times \varepsilon(x,t) \tag{1}$$

Where: APAR(x,t) represents the Absorbed Photosynthetically Active Radiation (APAR) for pixel x in month t, with units of MJ/m^2, and ϵ(x,t) denotes the actual light use efficiency for pixel x in month t, expressed in units of gC/MJ.

(1) APAR Estimation: The calculation formula is as follows:

$$\mathrm{APAR}(x,t) = \mathrm{SOL}(x,t) \times \mathrm{FPAR}(x,t) \times 0.5 \tag{2}$$

Where: SOL(x,t) represents the total solar radiation actually incident on the surface at pixel x in month t, with units of MJ/m^2, and FPAR(x,t) denotes the effective absorption ratio of total solar radiation by vegetation at pixel x in month t. The constant 0.5 represents the ratio of photosynthetically active radiation to total solar radiation.

$$\mathrm{FPAR}(x,t) = (\mathrm{FPAR}(x,t)_{\mathrm{NDVI}} + \mathrm{FPAR}(x,t)_{\mathrm{SR}})/2 \tag{3}$$

$$\mathrm{FPAR}(x,t)_{\mathrm{NDVI}} = \frac{(\mathrm{NDVI}(x,t) - \mathrm{NDVI}_{i,min}) \times (\mathrm{FPAR}_{max} - \mathrm{FPAR}_{min})}{\mathrm{NDVI}_{i,max} - \mathrm{NDVI}_{i,min}} + \mathrm{FPAR}_{min} \tag{4}$$

$$\mathrm{FPAR}(x,t)_{\mathrm{SR}} = \frac{(\mathrm{SR}(x,t) - \mathrm{SR}_{i,min}) \times (\mathrm{FPAR}_{max} - \mathrm{FPAR}_{min})}{\mathrm{SR}_{i,max} - \mathrm{SR}_{i,min}} + \mathrm{FPAR}_{min} \tag{5}$$

$$\mathrm{SR}(x,t) = \frac{1 + \mathrm{NDVI}(x,t)}{1 - \mathrm{NDVI}(x,t)} \tag{6}$$

Where: FPAR(x,t)NDVI and FPAR(x,t)SR are the vegetation layer's absorption proportions of photosynthetically active radiation at pixel x in month t, calculated through NDVI and SR, respectively. NDVI(x,t) and SR(x,t) represent the Normalized Difference Vegetation Index (NDVI) and Simple Ratio (SR) values for pixel x in month t. $FPAR_{max}$ = 0.95 and $FPAR_{min}$ = 0.001 are employed as independent parameters. $NDVI_{i,max}$ and $NDVI_{i,min}$ represent the maximum and minimum NDVI values for the i-th vegetation type, while $SR_{i,min}$ and $SR_{i,max}$ denote the minimum and maximum SR values for the i-th vegetation type.

(2) Estimation of Actual Light Use Efficiency (ε)

In vegetation productivity research, the actual light use efficiency is significantly influenced by temperature, water availability, and vegetation type. The calculation formula is as follows:

$$\varepsilon(x,t) = T_{\varepsilon 1}(x,t) \times T_{\varepsilon 2}(x,t) \times W_{\varepsilon}(x,t) \times \varepsilon_{max} \tag{7}$$

Where, $T_{\varepsilon1}$(x,t) and $T_{\varepsilon2}$(x,t) represent the stress coefficients of maximum temperature (T_{max}) and minimum temperature (T_{min}) on the actual light use efficiency ε(x,t). Wε denotes the water stress coefficient, and ε_{max} represents the maximum light use efficiency of vegetation under ideal conditions.

$$T_{\varepsilon1}(x,t) = 0.8 + 00.2 \times T_{opt}(x) - 0.005 \times \left[T_{opt}(x)\right]^2 \tag{8}$$

$$T_{\varepsilon2}(x,t) = \frac{1.184}{1+\exp[0.2\times T_{opt}(x)-10-T(x,t)]} \times \frac{1}{1+\exp[0.3\times(-T_{opt}(x)-10+T(x,t))]} \tag{9}$$

Where, $T_{\varepsilon1}(x,t)$ represents the reduction in net primary productivity due to the intrinsic biochemical constraints of plants at low and high temperatures. $T_{opt}(x)$ is the optimal temperature for plant growth, defined as the average monthly temperature of the month when NDVI reaches its highest value in a given region (°C). When the monthly average temperature T(x,t) is less than or equal to -10°C, $T_{\varepsilon1}(x,t)$ is set to 0.

$T_{\varepsilon2}(x,t)$ represents the gradual decline in light use efficiency as temperatures deviate from the optimal temperature $T_{opt}(x)$ toward higher or lower ranges. When the monthly average temperature T(x,t) is either 10°C above or 13°C below the optimal temperature, the $T_{\varepsilon2}(x,t)$ value is reduced to half of its value at the optimal temperature.

(3) Maximum Light Use Efficiency (ε_{max})

In optimal growth environments, when excluding temperature and water stress influences, the maximum light use efficiency (ε_{max}) reflects the vegetation's maximum conversion capacity for photosynthetically active radiation. This parameter exhibits diversity due to variations in vegetation types and climatic conditions.

This study applied the CASA model to integrate vegetation coverage data, NDVI spatiotemporal sequences, and meteorological observation records. NDVI maximum and minimum thresholds, along with corresponding solar radiation maximum and minimum values, were calculated separately for different vegetation functional types.

During the ε_{max} parameter configuration process, the research referenced the simulation results of maximum light use efficiency for typical Chinese vegetation by Zhu Wenquan,[17] which was based on the NPP remote sensing estimation model and least squares method. The parameter values are presented in Table 1, ensuring the scientific rigor and applicability of model parameter settings. This parameter optimization approach contributes to improving the estimation accuracy of terrestrial ecosystem net primary productivity.

Table 1 Maximum light energy utilization rate of different vegetation types

Vegetation Type	Broad-leaved Forest	Needle-leaved Forest	Mixed Forest	Shrubland	Grassland	Cropland	Wetland	Barren Land
Light Use Efficiency	0.692	0.476	0.768	0.429	0.542	0.542	0.542	0.389

3. Results

3.1. Validation of NPP results

In the process of data analysis, ensuring accuracy and reliability is a fundamental prerequisite for scientific research. Given the extensive spatial coverage of the study area, directly obtaining comprehensive net primary productivity (NPP) field measurements presents significant challenges. In recent years, the Carnegie-Ames-Stanford Approach (CASA) model has been widely applied for regional NPP estimation; however, the accuracy of model-generated data requires rigorous validation.

Consequently, this study employs a methodological approach to verify the reliability of CASA model-derived NPP data. Specifically, we utilized MOD12Q1 model-generated NPP data series for model fitting and cross-validation. The NPP data from the MOD12Q1 model were sourced from 500 randomly distributed sampling points, while the CASA model NPP values were calculated using light use efficiency algorithms. The fitting results will ultimately serve to authenticate and evaluate the accuracy of the CASA model-generated datasets.

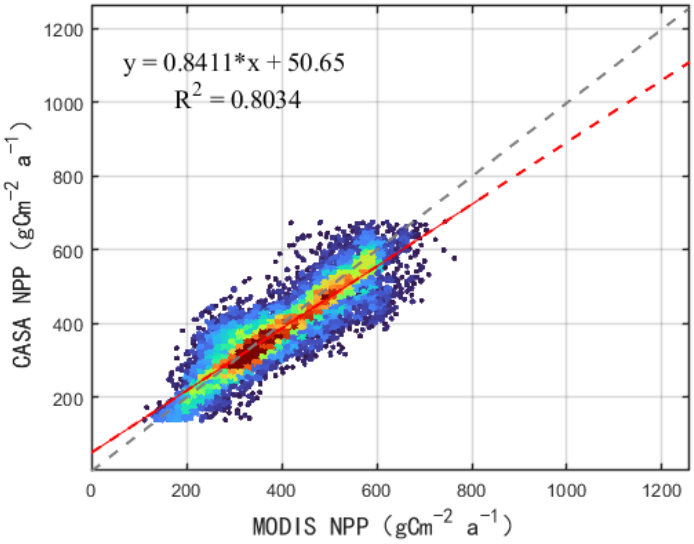

Fig. 1 Accuracy verification of vegetation NPP estimation

Based on Fig. 1. after fitting the NPP data generated by the MOD12Q1 and CASA models, we observed a linear correlation between the two data products at the pixel scale. The fitting function y = 0.8411x + 50.65 indicates a strong positive correlation between the two models. Furthermore, the coefficient of determination (R^2 = 0.8034) demonstrates a high statistical consistency across the two model-derived datasets. This result validates the feasibility of using the CASA model for regional-scale NPP estimation and supports its application in subsequent research investigations.

3.2. .Time series variation of vegetation NPP

Analysis of the annual mean Net Primary Productivity (NPP) in the Northeast Forest-Grassland Ecotone from 2000 to 2023 revealed a comprehensive vegetation productivity change curve (Fig. 2). The annual NPP values ranged between 265.31 and 423.52 $gC{\cdot}m^{-2}{\cdot}a^{-1}$, with an overall mean of 359.35 $gC{\cdot}m^{-2}{\cdot}a^{-1}$. The highest NPP was recorded in 2023 at 423.52 $gC{\cdot}m^{-2}{\cdot}a^{-1}$, representing a 17.8% increase from the mean, while the lowest value of 265.31 $gC{\cdot}m^{-2}{\cdot}a^{-1}$ occurred in 2000, which was 26.17% below the mean.

A detailed examination of the NPP trajectory showed a substantial increase from 265.31 $gC{\cdot}m^{-2}{\cdot}a^{-1}$ in 2000 to 423.52 $gC{\cdot}m^{-2}{\cdot}a^{-1}$ in 2023, representing a significant growth of 59.63%. This equates to an average annual increment of approximately 6.59 $gC{\cdot}m^{-2}{\cdot}a^{-1}$, indicating a progressive enhancement of vegetation net primary productivity in the region.

The linear regression model y = 5.532x − 10769.931 demonstrates a strong linear correlation between NPP values and temporal progression. The coefficient of determination (R^2 = 0.764) suggests a robust model fit, providing confidence in the observed trend and potential for future vegetation productivity projections.

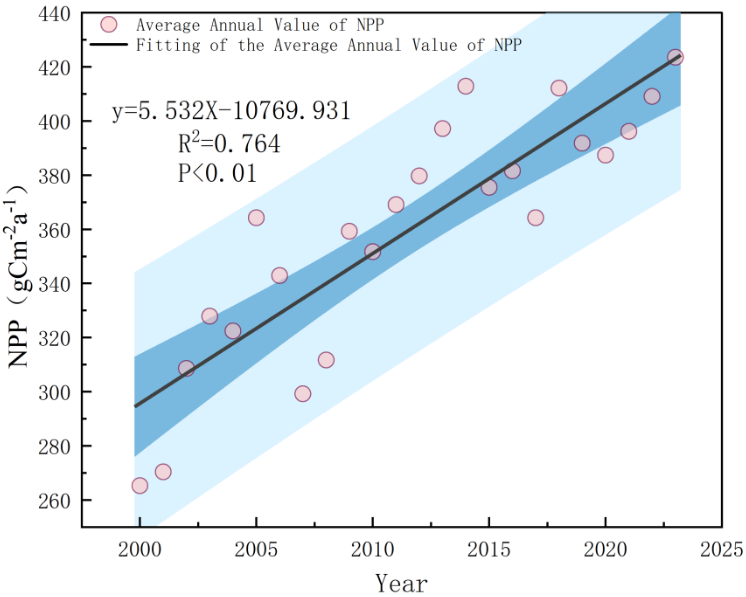

Fig. 2 Interannual NPP changes of vegetation from 2000 to 2023

3.3. .Spatial distribution characteristics of vegetation NPP

The Northeast Forest-Grassland Ecotone encompasses six administrative regions from north to south: Hulunbuir City, Xingan League, Tongliao City, Chifeng City, Chengde City, and Zhangjiakou City. This study employs an administrative city-level approach to analyze the annual mean vegetation Net Primary Productivity (NPP) within each administrative region, quantified in carbon content (C). The NPP values were categorized into five gradient ranges: - 0~150 gC·m^{-2}·a^{-1}, - 150~300 gC·m^{-2}·a^{-1}, - 300~450 gC·m^{-2}·a^{-1}, - 450~600 gC·m^{-2}·a^{-1}, - >600 gC·m^{-2}·a^{-1}. This methodological approach aims to provide a scientific and comprehensive exploration of the spatial distribution characteristics of vegetation NPP in the study region.

Analysis of the multi-year mean vegetation Net Primary Productivity (NPP) spatial distribution map (Fig. 3) reveals a complex pattern of vegetation productivity influenced by zonal characteristics, longitude, and comprehensive topoclimatic factors. The spatial extent of areas with NPP < 300 gC·m^{-2}·a^{-1} significantly exceeds regions with NPP > 300 gC·m^{-2}·a^{-1}, indicating that most of the study area supports vegetation at moderate to low productivity levels.

The spatial distribution of vegetation NPP demonstrates a patch-like transition from south to north, with a notable vertical gradient where average annual NPP increases with elevation, manifesting a north-high, south-low distribution pattern. At the administrative region scale: Southwestern Hulunbuir City, most of Tongliao City, central-eastern Chifeng City, and southeastern Xingan League exhibit the lowest NPP range of 0~150 gC·m^{-2}·a^{-1}., Hulunbuir City and most of Chengde City show significantly higher NPP values exceeding 450 gC·m^{-2}·a^{-1}.

These disparities can be attributed to region-specific factors, including: Unique climatic conditions, Vegetation type variations, Differential land use practices.

The spatially explicit data comprehensively illustrates the heterogeneity of vegetation NPP in the Northeast Forest-Grassland Ecotone. By delineating the carbon sequestration potential across different territories, this analysis provides crucial scientific insights for targeted regional ecological restoration strategies.

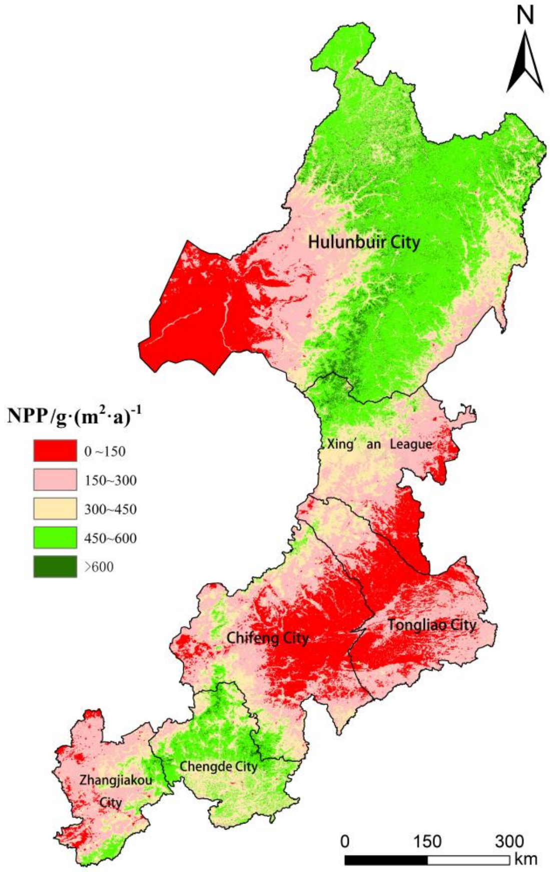

Fig. 3 Spatial distribution map of vegetation NPP multi-year average in each city

4. Conclusion

The spatiotemporal dynamics of Net Primary Productivity (NPP) in the Northeast Forest-Grassland Ecotone reveal complex ecosystem responses to environmental changes during 2000-2023. Our multiscale analysis utilizing meteorological, vegetation spatial distribution, and remote sensing datasets through the CASA model provides critical insights into regional ecological transformation.

The longitudinal trajectory of vegetation NPP demonstrates a nuanced evolutionary pattern characterized by significant growth and distinctive developmental stages. The cumulative NPP increment of 59.63% reflects substantial ecological resilience, with three notable phases: an accelerated growth period (2000-2014) marked by a 55.60% increase, a transient recession (2014-2017) with an 11.76% decline, and a steady recovery phase (2017-2023) exhibiting a 16.25% resurgence . These findings underscore the dynamic nature of ecosystem productivity and suggest progressive environmental rehabilitation in this critical ecological transition zone.

Spatially, the NPP distribution manifests pronounced heterogeneity, presenting a north-high, south-low gradient with a regional mean of 339.13 $gC·m^{-2}·a^{-1}$. Significant inter-regional variations are evident, with Chengde and Hulunbuir emerging as high-productivity zones, contrasting sharply with the low-productivity Tongliao region. The NPP maximum value escalated from 883.75 to 1150.34 $gC·m^{-2}·a^{-1}$, revealing asymmetric spatial dynamics influenced by complex hydrothermal conditions, vegetation composition, and anthropogenic interventions .

The significance analysis further illuminates intricate spatiotemporal patterns: 91.84% of the studied area demonstrated NPP increments, with 12.07% exhibiting statistically significant increases predominantly concentrated in the Hulunbuir Plateau and central administrative regions. Notably, only 8.16% of the area experienced productivity decline. The spatial configuration reveals a centrally concentrated significant increase (26.31%), while northern and southern peripheries predominantly exhibit stable characteristics (53.59%).

These findings not only contribute to our understanding of regional ecological dynamics but also provide critical scientific foundations for targeted ecological restoration strategies. Future research should focus on disentangling the complex interactions between climate change, land use transformation, and ecosystem productivity to develop more sophisticated predictive models.

Acknowledgements

We would like to thank editage (www. editage. com) for English language editing. We also thank the anonymous reviewers and editors for their valuable, constructive comments.

References

[1] Cannell M G R, Milne R, Hargreaves K J, et al. National inventories of terrestrial carbon sources and sinks: the UK experience. Climatic Change,42 (1999):505-530.

[2] Allen, Myles R., et al. "Geological Net Zero and the need for disaggregated accounting for carbon sinks." Nature (2024): 1-3.

[3] Luo, Qing, et al. "Unexpected response of terrestrial carbon sink to rural depopulation in China." Science of The Total Environment 948 (2024): 174595.

[4] Song, Shixiong, et al. "Study on carbon sink of cropland and influencing factors: A multiscale analysis based on geographical weighted regression model." Journal of Cleaner Production 447 (2024): 141455.

[5] Li, "The impact of landscape spatial morphology on green carbon sink in the urban riverfront area." Cities 148 (2024): 104919.

[6] Aruhan, and Dongchang Liu. "Study on the influencing factors of the evolution of space pattern based on principal component analysis in Duolun County." Scientific Reports 14.1 (2024): 20567.

[7] Zhao, Dan, et al. "Nature-based solutions: Assessing the carbon sink potential and influencing factors of urban park plant communities in the temperate monsoon climate zone." Science of The Total Environment 950 (2024): 175347.

[8] Wei, Xuezhi, and Quansheng Wang. "Policy suggestions for tap** the potential of ocean carbon sinks in the context of “double carbon” goals in China." Frontiers in Marine Science 11 (2024): 1298372.

[9] Afzali, Afsaneh, et al. "Investigating net primary production in climate regions of Khuzestan Province, Iran using CASA model." International Journal of Biometeorology 68.7 (2024): 1357-1370.

[10] Ruhan, A., Dongchang Liu. "Research on the carrying capacity of production, living and ecological space and its coupling coordination in Duolun County, Inner Mongolia." PloS one 19.12 (2024): e0309615.

[11] Potter, Christopher, and Stephanie Pass. "Changes in the net primary production of ecosystems across Western Europe from 2015 to 2022 in response to historic drought events." Carbon Balance and Management 19.1 (2024): 32.

[12] Cai, Yiling, et al. "Human activities significantly impact China’s net primary production variation from 2001 to 2020." Progress in Physical Geography: Earth and Environment 48.2 (2024): 251-274.

[13] Tang, Huan, Jiawei Fang, and **g Yuan. "Climate change and Land Use/Land Cover Change (LUCC) leading to spatial shifts in net primary productivity in Anhui Province, China." PloS one 19.9 (2024): e0307516.

[14] Zhao, Wenhui, et al. "Near-infrared radiance of vegetation is more sensitive than vegetation indices for monitoring NPP of winter wheat under water stress." IEEE Journal of Selected Topics in Applied Earth Observations and Remote Sensing (2024).

[15] Lieth H. Modelling the primary productivity of the world. Nature and Resources, 1972, 8:5-10.

ISSN: 1813-4890

[16] UCHIJIMA Z, SEINO H. Agroclimatic evaluation of net primary productivity of natural vegetations(1) Chikugo model for evaluating net primary productivity[J].Journal of Agricultural Meteorology,40(4) (1985), 343-352.

[17] Ji, Shu, et al. "Improved CASA-Based Net Ecosystem Productivity Estimation in China by Incorporating Developmental Factors into Autumn Phenology Model." Remote Sensing 17.3 (2025): 487.

[18] W.Q. Zhu. Simulation of maximum light use efficiency of typical vegetation in China Science Bulletin, 06 (2006), 700-706.